

Automatic Microaneurysm Detection from Non-dilated Diabetic Retinopathy Retinal Images

Akara Sopharak, Bunyarit Uyyanonvara, Sarah Barman and Tom Williamson

Abstract— Microaneurysms are the first clinical sign of diabetic retinopathy. The number of microaneurysms is used to indicate the severity of the disease. Early microaneurysm detection can help reduce the incidence of blindness. This paper investigates a set of optimally adjusted morphological operators used for microaneurysm detection on non-dilated pupil and low-contrast retinal images. The detected microaneurysms are validated by comparing with ophthalmologists' hand-drawn ground-truth. As a result, the sensitivity, specificity, precision and accuracy were 81.61, 99.99, 63.76 and 99.98%, respectively.

Index Terms— diabetic retinopathy, microaneurysms.

I. INTRODUCTION

Diabetic retinopathy (DR) is the most common cause of blindness in people of working age. The global prevalence of diabetes is expected to rise to 4.4% of the global population by 2030 [1]. An effective treatment to prevent vision loss is available, but diabetic retinopathy is asymptomatic until late in the disease process. The screening of diabetic patients for the development of diabetic retinopathy can reduce the risk of blindness by 50% [2]-[4]. With a large number of patients, the number of ophthalmologists is not sufficient to cope with all patients, especially in rural areas or if the workload of local ophthalmologists is substantial. Therefore, automated early detection could limit the severity of the disease and assist ophthalmologists in investigating and treating the disease more efficiently.

Microaneurysms (MA) are the earliest clinically localized characteristic of DR [5]. Their detection can be used to grade the DR stage as shown in Table. I [6].

A number of methods for MA detection have been published. T. Spencer et al. [7], M.J. Cree et al. [8] and A. Frame et al. [9] propose a mathematical morphology

technique to segment MA within fluorescein angiograms. J.H. Hipwell et al. [10] use Gaussian matched filters to retain candidate MA for classification. Gardner et al. [11] use a back propagation neural network on sub-images (20x20 or 30x30 pixel windows). C. Sinthanayothin et al. [12] propose an automated system of detection of diabetic retinopathy using recursive region growing segmentation (RRGS). D. Usher et al. [13] employ a combination of RRGS and adaptive intensity thresholding to detect candidate lesion regions and a neural network is used for classification. T. Walter et al. [14] propose a method based on diameter closing and kernel density estimation for automatic classification. B. Dupas et al. [6] use a diameter-closing to segment MA candidate regions and k-nearest neighbours (kNN) to classify MA. M. Niemeijer et al. [15] combine prior works by T. Spencer et al. [7] and A. Frame et al. [8] with a detection system based on pixel classification and new features are proposed. A kNN classifier was used in the final step.

Most techniques mention earlier work on fluorescein angiographies or color images taken on patients with dilated pupils in which the MA and other retinal features are clearly visible. The examination time and effect on the patient could be reduced if the detection system could succeed on images taken from patients with non-dilated pupils. However, the quality of these images will be worse and it greatly affects the performance of those mentioned algorithms.

Automatic MA detection on images acquired without pupil dilation is investigated in this work with the aim of providing decision support in addition to reducing the workload of ophthalmologists.

In our previous work, we have presented methods for automatic exudate detection using a mathematical morphological technique, a FCM clustering technique, a combination of FCM and mathematical morphology, a naive Bayesian classifier, a SVMs classifier and a nearest neighbor classifier [16]-[19]. To improve the overall ability of DR detection system, a MA detection method is proposed.

TABLE I
CRITERIA USED FOR GRADING DIABETIC RETINOPATHY

DR stage	
Grade 0 (no DR)	MA = 0 and H = 0
Grade 1 (mild)	$1 \leq MA \leq 5$ and $H = 0$
Grade 2 (moderate)	$5 < MA < 15$ or $0 < H \leq 5$
Grade 3 (severe)	$MA \geq 15$ or $H > 5$

MA = microaneurysm, H = haemorrhage

Manuscript received January xx, 2011; revised March XX, 2011.

A. Sopharak is with Faculty of Science and Arts, Burapha University, Chanthaburi Campus, 57 Moo 1, Kamong, Thamai, Chantaburi 22170, Thailand (phone: +66(0)39-310-000; e-mail: akara@buu.ac.th).

B. Uyyanonvara is with Sirindhorn International Institute of Technology, Thammasat University, 131 Moo 5, Tiwanont Road, Bangkadi, Muang, Pathumthani, 12000, Thailand (e-mail: bunyarit@siit.tu.ac.th).

S. A. Barman is with Kingston University, Penrhyn Road, Kingston Upon Thames, Surrey, KT1 2EE, United Kingdom (e-mail : S.Barman@kingston.ac.uk).

T. Williamson is with Department of Ophthalmology, St Thomas' Hospital, London, SE1 7EH, United Kingdom (e-mail : tom@retinasurgery.co.uk)

II. METHOD

All digital retinal images taken of patients with non-dilated pupils were obtained from a KOWA-7 non-mydratric retinal camera with a 45° field of view. The image size is 752 x 500 pixels with 24 bits per pixel. MAs are hard to detect because their contrast is very low and hardly visible and also difficult to distinguish from noise or pigmentation variations.

The proposed system has three main steps. The preprocessing step includes noise removal, contrast enhancement and shade correction. Candidate retinal features which may cause a false detection, i.e., exudates and vessels are detected in the second step. And the last step is MA detection by using a set of optimally adjusted mathematical morphology. The overall procedure of MA detection is shown in Fig. 1.

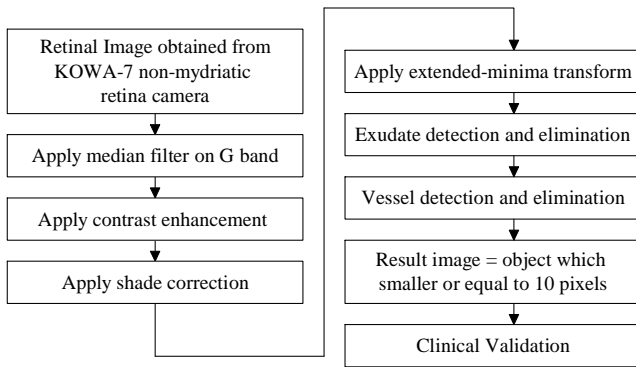


Fig. 1. Procedure of microaneurysm detection.

A. Preprocessing

A preprocessing step is needed to improve the image quality prior to the detection step. The green plane (f_g) of the original RGB color image was used as red lesions have the highest contrast with the background in this color plane [20]. A median filtering operation was applied on f_g to reduce noise before a Contrast Limited Adaptive Histogram Equalization was applied for contrast enhancement. A dark region (including noise and MAs) may dominate after contrast enhancement. To account for this a shade correction algorithm was applied to the green band in order to remove slow background variation due to non-uniform illumination. The original image in the RGB plane, the green band image, the green band image after removal of noise and contrast enhancement, and the shade corrected image (f_{sc}) are shown in Fig. 2 (a) through Fig. 2 (d).

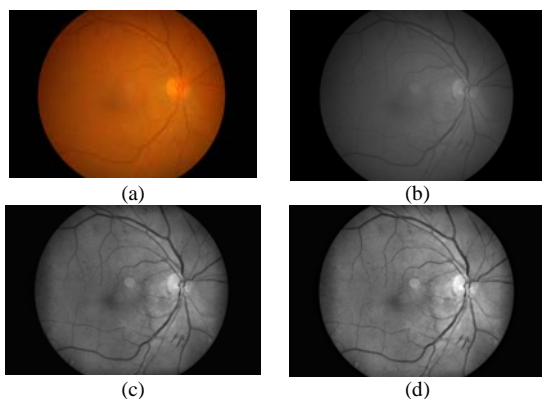


Fig. 2. Preprocessing steps. (a) Original RGB Image. (b) Green band. (c) Green band after contrast enhancement. (d) Shade corrected image.

B. Exudate Detection

MA detection is our main purpose, however we have to remove bright lesions such as exudates prior to the process because when they lie close together, small islands are formed between them and they can be wrongly detected as MAs. Mathematical morphological methods (proposed in our previous work [16]) was used due to its computationally low cost. Examples of exudate detection results overlaid on the original image are shown in Fig. 3.

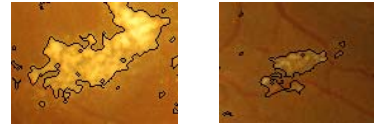


Fig. 3. Exudate detection results shown overlaid on original images.

C. Vessel Detection

Vessels are another element in the image that needs to be removed prior the MA detection since MA and vessels both appear in a reddish color and MAs cannot occur on vessels.

To detect vessels, two intermediate images are generated. The first image is obtained using a closing operator (ϕ) on image f_{sc} to eliminate the details from the image. A second image is obtained by filled-in small black dots on f_{sc} with diameters smaller than size of MA in order to remove small red objects and fill holes in the vessel. The diameter of a MA lies between 10 and 100 μm , but it always smaller then a diameter $\lambda < 125 \mu\text{m}$ [6]. In our image set of size 752 x 500 pixels, the size of a MA is about 10 pixels. Vessel candidate areas are obtained by the difference between the first image and the second image from the previous step. The closing image and filled in image are shown in Fig. 4 (a) and Fig. 4 (b).

$$f_{vesselDiff} = \phi^{(B_1)}(f_{sc}) - fill(f_{sc}) \quad (1)$$

where B_j is the morphological structuring element.

The candidate vessels were then thresholded at grey level α_l as in (2). Let $T = \{t_{min}, \dots, t_{max}\}$ be an ordered set of grey levels, we have

$$f_{vesselT} = T_{[\alpha_l, t_{max}]}(f_{vesselDiff}) \quad (2)$$

As a result shown in Fig. 4 (c), there are some small isolated objects left. The objects which have size smaller than 10 pixels (size of MA, as mentioned above) are then removed from $f_{vesselT}$. The result is shown in Fig. 4 (d).

D. Microaneurysm Detection

Retinal MAs are focal dilatations of retinal capillaries. They are discrete, localized saccular distensions of the weakened capillary walls and appear as small round dark red dots on the retinal surface.

According to the medical definition of MA [5], [6], it is a reddish, circular pattern with a diameter $\lambda < 125 \mu\text{m}$. We aim to find an MA by its diameter and isolated connected red

pixels with a constant intensity value, and whose external boundary pixels all have a higher value; in the green plane of a RGB image.

A preprocessed retinal image was used as preliminary image for MA detection. The extended-minima transform [21] is applied to the f_{sc} image. This transformation is a thresholding technique that brings most of the valleys to zero. The extended minima transform on the f_{sc} image with threshold value α_2 is shown in (3).

$$f_E = EM(f_{sc}, \alpha_2) \quad (3)$$

where f_E is the output image.

The selection of threshold is very important where the higher value of α_2 will lower the number of regions and a lower value of α_2 will raise the number of regions. The result is shown in Fig. 4 (e). The previous detected exudates and vessels were removed from the resulting image. The result is shown in Fig. 4 (f).

$$f_{VE_removed} = f_E - f_{vesselT} - f_{ex} \quad (4)$$

where f_{ex} is the exudate detected image.

Then the objects with a size smaller or equal to 10 pixels are selected and classified as MAs. The result is shown in Fig. 4 (g).

There are parameters used in this experiment. They are, namely, the size of structuring element (B_1) used for the closing operation, threshold values (α_1 and α_2). α_1 was calculated automatically using the Otsu algorithm. B_1 and α_2 were varied and tested in order to assess the algorithm performance in an experiment. Each parameter was varied as follows:

$$B_1 \in \{9, 10, 11, 12\}$$

$$\alpha_2 \in \{0.01, 0.03, 0.05, 0.07\}$$

All parameters in this proposed method are set using the values that gave highest sensitivity and specificity in the previous experiment. The experiment showed that the value of $B_1=10$ and $\alpha_2 = 0.05$ gave a good balance between the number of detected MAs and the number of detected spurious objects.

III. RESULTS

Data sets of 45 non-dilated retinal images are tested. Detected MAs are compared with the ophthalmologists' hand-drawn ground-truth images for verification. Sensitivity is the percentage of the actual MA pixels that are detected, and specificity is the percentage of non-MA pixels that are correctly classified as non-MA pixels. Precision is the percentage of detected pixels that are actually MAs. Accuracy is the overall per-pixel success rate of the classifier.

Sensitivity, specificity, precision and accuracy in this experiment are 81.61, 99.99, 63.76 and 99.98%, respectively. The numbers of MAs are also counted for automated grading of the severity of the DR. Example resulting images of MA detection are shown in Fig. 5.

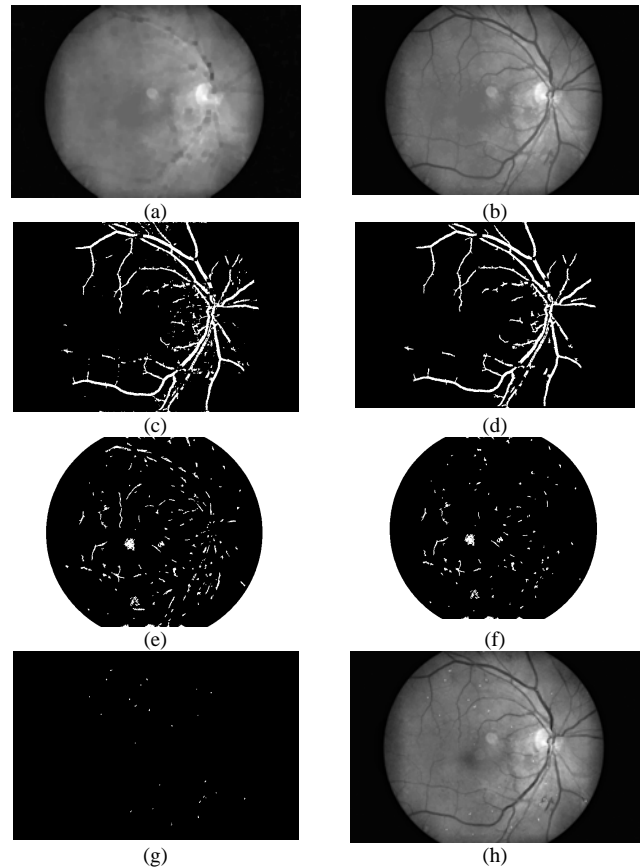


Fig. 4. Microaneurysm detection (a) Image after closing (b) Filled-in image (c) Difference image (d) Image after removal of object smaller than the size of microaneurysm from image (c) (e) Extended-minima transform image (f) Image after removal of vessels (g) Detected microaneurysms (h) Microaneurysms superimposed on original image.

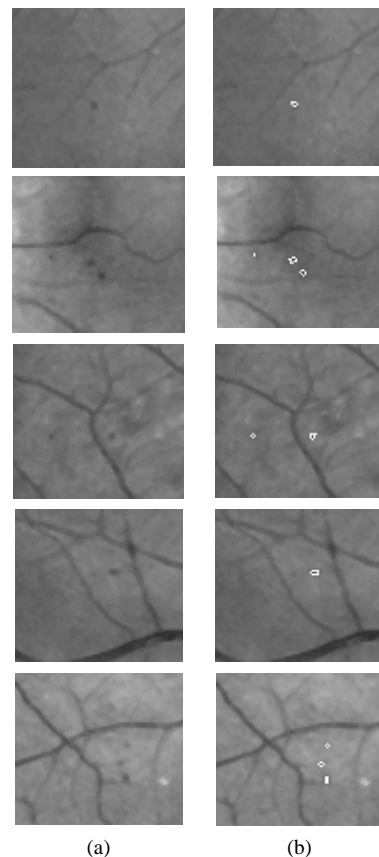


Fig. 5. Example of microaneurysm detection results. (a) Original images. (b) Detected results.

IV. CONCLUSION AND DISCUSSION

Our work concentrates on microaneurysm detection from diabetic retinopathy patient's non-dilated pupil digital images. It is an extension to our previously proposed automated DR screening system. The system intends to help the ophthalmologists in the diabetic retinopathy screening process to detect symptoms faster and more easily. The algorithm could detect MAs on very poor quality images. Although further development of this algorithm is still required, the results are satisfying. The outcome is quite successful with sensitivity and specificity of 81.61% and 99.99%, respectively. The system also provided ophthalmologists with the number of MAs for grading the DR stage. In order to apply to a clinical application, the proposed method will be combined with an exudate detection system.

ACKNOWLEDGMENT

This research is funded by the Burapha University, Chanthaburi Campus.

REFERENCES

- [1] S. Wild, G. Roglic, A. Green et al., "Global prevalence of diabetes: estimates for the year 2000 and projections for 2030," *Diabetes Care* 27, 2004, pp.1047-1053.
- [2] W. Hsu, P.M.D.S Pallawala, Mong Li Lee et al., "The Role of Domain Knowledge in the Detection of Retinal Hard Exudates," In *Proceedings of the 2001 IEEE Computer Society Conference on Computer Vision and Pattern Recognition* 2, 2001, pp.II-246 - II-251.
- [3] A. Osareh, M. Mirmehdi, B. Thomas and R. Markham, "Automated Identification of Diabetic Retinal Exudates in Digital Colour Images," *British Journal of Ophthalmology* 87(10), 2003, pp.1220-1223.
- [4] C.I. Sanchez, R. Hornero, M.I. Lopez et al., "Retinal Image Analysis to Detect and Quantify Lesions Associated with Diabetic Retinopathy," In *Proceedings of 26th IEEE Annual International Conference on Engineering in Medicine and Biology Society (EMBC)* 1, 2004, pp.1624 - 1627.
- [5] P. Massin, A. Erginay, and A. Gaudric, "Retinopathie Diabetique", Elsevier, Editions scientifiques de medicales, Elsevier, SAS, Paris 2000.
- [6] B. Dupas, T. Walter, A. Erginay et al., "Evaluation of automated fundus photograph analysis algorithms for detecting microaneurysms, haemorrhages and exudates, and of a computer-assisted diagnostic system for grading diabetic retinopathy," *Diabetes & Metabolism* 36(3), 2010, pp. 213-220.
- [7] T. Spencer, J.A. Olson, K.C. McHardy et al., "An image-processing strategy for the segmentation and quantification of microaneurysms in fluorescein angiograms of the ocular fundus," *Comp Biomed Res* 29, 1996, pp. 284-302.
- [8] M.J. Cree, J.A. Olson, K.C. McHardy et al., "A fully automated comparative microaneurysm digital detection system," *Eye* 11, 1997, pp. 622-628.
- [9] A. Frame, P. Undrill, M. Cree et al., "A comparison of computer based classification methods applied to the detection of microaneurysms in ophthalmic fluorescein angiograms," *Comput. Biol. Med.* 28, 1998, pp. 225-238.
- [10] J.H. Hipwell, F. Strachan, J.A. Olson et al., "Automated detection of microaneurysms in digital red-free photographs: a diabetic retinopathy screening tool," *Diabetic Medicine* 17, 2000, pp.588-594.
- [11] G. Gardner, D. Keating, T.H. Williamson et al., "Automatic detection of diabetic retinopathy using an artificial neural network: a screening tool," *Br J Ophthalmol* 80, 1996, pp.940-944.
- [12] C. Sinthanayothin, J.F. Boyce, T.H. Williamson, T.H. et al., "Automated Detection of Diabetic Retinopathy on Digital Fundus Image," *Diabetic Medicine* 19(2), 2002, pp. 105-112, 2002.
- [13] D. Usher, M. Dumskyj, M. Himaga et al., "Automated Detection of Diabetic Retinopathy in Digital Retinal Images: A Tool for Diabetic Retinopathy Screening," *Diabetic Medicine* 21(1), 2004, pp. 84-90.
- [14] T. Walter, P. Massin, A. Erginay et al., "Automatic detection of microaneurysms in color fundus images," *Medical Image Analysis* 11(6), 2007, pp.555-566.
- [15] M. Niemeijer, B. van Ginneken, J. Staal et al., "Automatic detection of red lesions in digital color fundus photographs," *IEEE Trans Med Imaging* 24(5), 2005, pp.584-592.
- [16] A. Sopharak, B. Uyyanonvara, S. Barman et al., "Automatic detection of diabetic retinopathy exudates from non-dilated retinal images using mathematical morphology methods," *Computer Medical Imaging and Graphics* 32(8), 2008, pp. 720-727.
- [17] A. Sopharak, B. Uyyanonvara, and S. Barman, "Automatic exudate detection from non-dilated diabetic retinopathy retinal images using fuzzy C-means clustering," *Sensors* 9(3), 2009, pp. 2148-2161.
- [18] A. Sopharak, M. Dailey, B. Uyyanonvara et al., "Machine Learning Approach to Automatic Exudate Detection in Retinal Images from Diabetic Patients," *Journal of Modern Optics* 57(2), 2010, pp. 124 - 135.
- [19] A. Sopharak, B. Uyyanonvara, S. Barman et al., "Comparative Analysis of Automatic Exudate Detection Algorithms," In *Proceedings of the International Conference on Signal and Image Engineering (ICSIE)*, 2010, pp.738-741.
- [20] Hoover, V.Kouznetsova, and M.Goldbaum, "Locating blood vessels in retinal images by piecewise threshold probing of a matched filter response," *IEEE Trans. Med. Imag.* 19(3), 2000, pp. 203-210.
- [21] P. Soille, *Morphological Image Analysis: Principles and Applications*, Springer-Verlag, 1999, pp. 170-171.